Manuscript SREP-12-04080

SUPPLEMENTARY INFORMATION

Red coral extinction risk enhanced by ocean acidification

Carlo Cerrano, Ulisse Cardini, Silvia Bianchelli, Cinzia Corinaldesi,

Antonio Pusceddu, Roberto Danovaro*

Department of Life and Environmental Sciences,

Polytechnic University of Marche, Ancona, Italy

*Corresponding author:

e-mail: r.danovaro@univpm.it

Telephone: (+39) 071 2204654

Fax: (+39) 071 2204650

Section 1 - The target species

Among precious corals, the most valuable species are red and pink corals of the genus *Corallium* in the order Gorgonacea. *Corallium* species are found worldwide in tropical, subtropical and temperate oceans[1], including five species in the Atlantic, two from the Indian Ocean, three from the eastern Pacific Ocean, and 15 from the Western Pacific Ocean[2]. Because of their bathymetric range, habitat preference and ecological role, precious corals belong to the functional group called "structure-forming deep corals"[3]. However, deep-sea organisms are generally defined as those occurring deeper than the continental shelf, whereas the term "deep corals" refers to corals that are neither shallow water corals nor entirely deep-sea organisms. Precious corals are important keystone species in various marine ecosystems because they provide 3D complexity to habitats, structuring and stabilizing the ecosystem[4] and thus significantly increasing biodiversity.

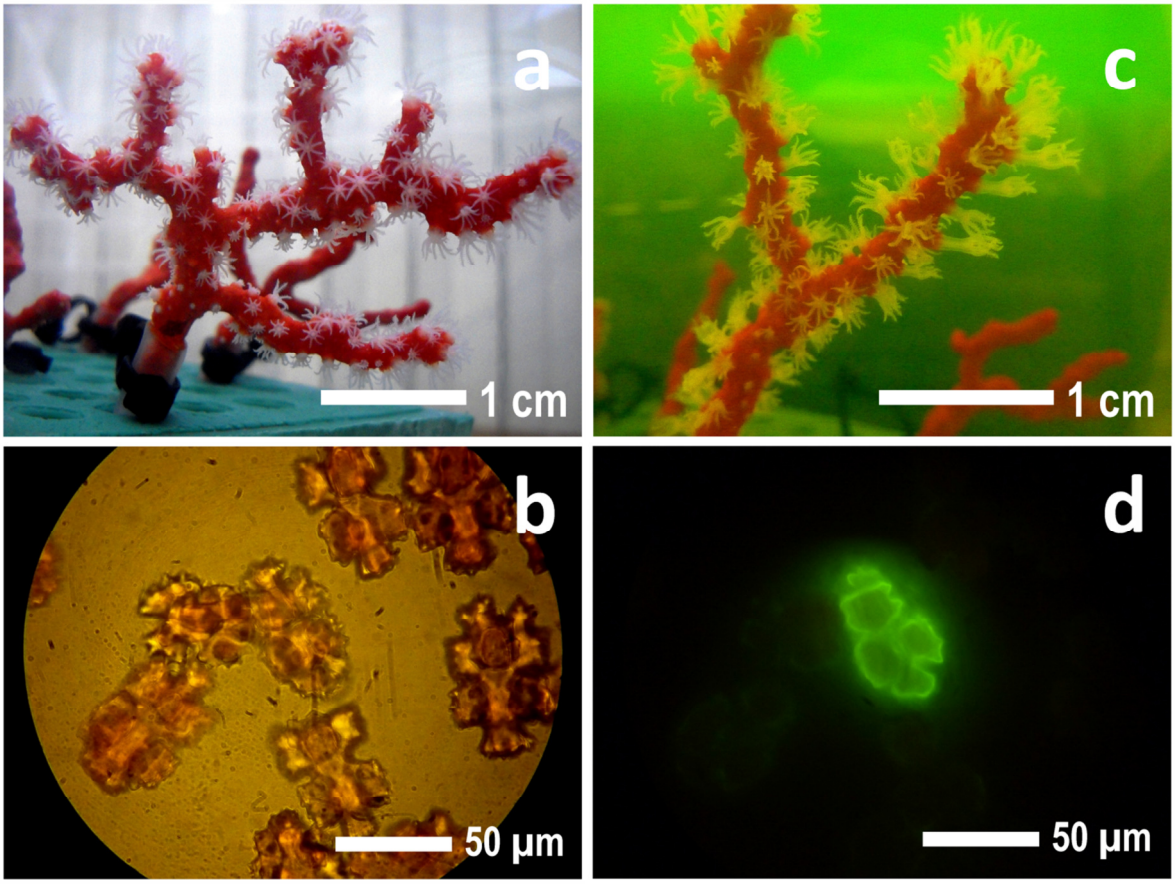

Figure S1. Red coral branches in the experimental mesocosms: before (a) and after (c) the inoculation of calcein; sclerites from the apices under the epifluorescence microscope: total (b) and newly-accreted ones (because visible under 450–490 nm excitation filter, d).

The red coral (*Corallium rubrum*, L. 1758; Figure S1) is one of the key ecosystem engineering species of Mediterranean coralligenous assemblages[5]. *C. rubrum* is one of the most long-lived

inhabitants of the coralligenous, possibly living for approximately 200 years[6]. It is a sciaphilous species that can be found in depths from 5 to 800 m[7]. The precious axial skeleton has tree-like growth form and can reach sometimes more than 50 cm in height and several centimetres in diameter[1]. Axial skeleton and sclerites are built of a composite material with an inorganic fraction of calcium carbonate crystallized under the form of high magnesian calcite (3.44% Mg[8]) and an organic matrix[9] rich in carotenoids, responsible of the red pigmentation[10]. From biomimetic experiments, it has been suggested that the organic matrix plays a role as an assembler of carbonate blocks, forming mesocrystals[11,12]. Sclerites are present in two different shapes (crosses and capstans[13], Figure S1) and in high amount within the mesoglea, and can reach about 10^6 sclerites mg^{-1} tissue proteins[14]. The sclerites are initially formed in intracellular vesicles within scleroblasts present in the mesoglea[15]. The axial skeleton of the red coral results first from the fusion of sclerite-like structures at the apex of the colony, and then from an extracellular concentric secretion by the skeletogenic epithelium[16]. Moreover, the sclerites in the apices represent the most important site of $CaCO_3$ deposition in comparison with axial skeleton and tissue[14].

For these reasons, reduction in calcification of *C. rubrum* in response to increased pCO_2 was investigated by using calcein as a tracer to recognize newly-accreted sclerites in the apical part of the red coral branches after 120 hours labeling under controlled vs. acidified conditions (Figure S1).

Section 2 - Physical-chemical variables and carbonate parameters during the experiments

Physical-chemical variables and carbonate system parameters at the beginning and the end of the experiment in the three treatments are summarized in Table S1. Values of pH in the mesocosms did not vary significantly from those measured in the field at the sample collection site (t-Test P>0.05 for all contrasts) during the acclimation period, but significantly varied in the two treatments once bubbling was initiated (t-Test P<0.001 for all contrasts). pH values in both acidified treatments significantly dropped few hours after the beginning of bubbling and then remained almost constant during the entire duration of the experiment (Figure S2). Total Alkalinity was measured through an open-cell potentiometric titration procedure calibrated with certified standards[17]. Alkalinity measures fall into values recorded for the Western Mediterranean Sea[18]. Moreover, total alkalinity is known to decrease with the precipitation of calcium carbonate[19]. As a result, the noticed a non significant change in alkalinity is associated with the process of calcification in *C. rubrum*, which occurred both in the control and in the treatments, even if at different rates.

Table S1. Physical-chemical variables (Sal, T, pH_{NBS} and TA) and main carbonate parameters (DIC, pCO_2, HCO_3^-, Ω_{Ar}, Ω_{Ca}) at the sampling site and in the three experimental assets, at the start and at the end of the experiment. All numbers are mean values (n = 3) ± standard deviations. DIC, pCO_2, HCO_3^-, aragonite (Ω_{Ar}) and calcite (Ω_{Ca}) saturation state were calculated according to the method given in the text.

Treatment		Sal	T (°C)	pH_{NBS}	TA (µmol kg^{-1})	DIC (µmol kg^{-1})	pCO_2 (µatm)	HCO_3^- (µmol kg^{-1})	Ω_{Ar}	Ω_{Ca}
In situ		38.1 ±0.1	13.6 ±0.4	8.072 ±0.008	2576.3 ± 3.3	2321.9 ± 3.1	428.0 ±0.6	2120.3 ± 2.8	2.76 ± 0.01	4.29 ± 0.01
Control (pH 8.08)	start	38.1 ±0.3	13.37 ± 0.06	8.156 ± 0.015	2839.3 ± 23.5	2687.0 ± 23.5	838.1 ±44.0	2526.7 ± 23.4	1.97 ± 0.08	2.85 ± 0.11
	end	38.4 ± 0.1	13.60 ±0.13	8.052 ± 0.015	2380.0 ± 15.8	2198.9 ± 14.8	568.8 ± 10.0	2045.4 ±14.0	2.04 ± 0.04	2.96 ± 0.06
750 ppm (pH 7.88)	start	38.0 ±0.0	13.47 ±0.06	7.966 ± 0.006	2864.1 ± 34.9	2714.0 ± 34.0	857.3 ± 24.4	2553.5 ± 32.4	1.96 ± 0.05	2.84 ± 0.07
	end	38.7 ±0.1	13.50 ±0.01	7.915 ± 0.036	2304.4 ± 30.9	2172.4 ±39.6	733.9 ± 6.0	2042.6 ± 41.3	1.59 ± 0.07	2.31 ± 0.10
1000 ppm (pH 7.77)	start	38.1 ± 0.1	13.40 ±0.01	7.778 ± 0.010	2800.8 ±38.8	2649.7 ± 29.5	826.5 ± 30.6	2491.6 ±24.3	1.94 ± 0.10	2.81 ± 0.15
	end	38.4 ± 0.1	13.66 ±0.02	7.732 ± 0.053	2350.2 ±31.8	2249.5 ± 37.2	928.3 ± 56.9	2127.3 ± 37.7	1.36 ± 0.05	1.97 ± 0.07

Carbonate parameters perfectly reflects the effect of increased pCO_2 in the two acidified treatments[20], determining a sharp reduction of average Ω_{arag}, Ω_{calc} and CO_3^{2-}, and an increase in

DIC, $[CO_2]$, HCO_3^-, pCO_2, fCO_2 (Table S2). Anyway, experimental waters remained always oversaturated both for aragonite and for calcite. Recent studies suggest that moderate increases in inorganic nutrients may help the corals to offset the negative impact of ocean acidification[21,22]. Dissolved inorganic nutrients (PO_4^{3-}, SiO_2, NO_2^-, NO_3^-, NH_3/NH_4^+) concentrations in the mesocosms were determined at the beginning and the end of the experiment using an auto-analyzer. These analyses, integrated with the analysis of and Ca^{2+}, reveal that concentrations of nitrates and ammonia did not vary or even decreased during the experiment (Figure S3).

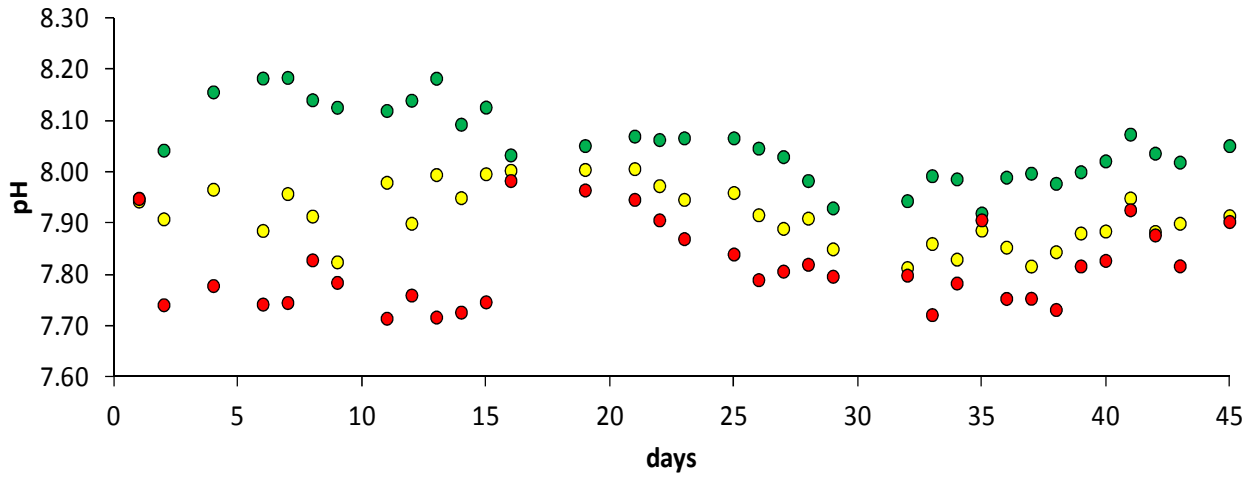

Figure S2. Daily pH values in mesocosms during the entire experiment. Green = pH 8.08 (control); yellow = pH 7.88; red = pH 7.77.

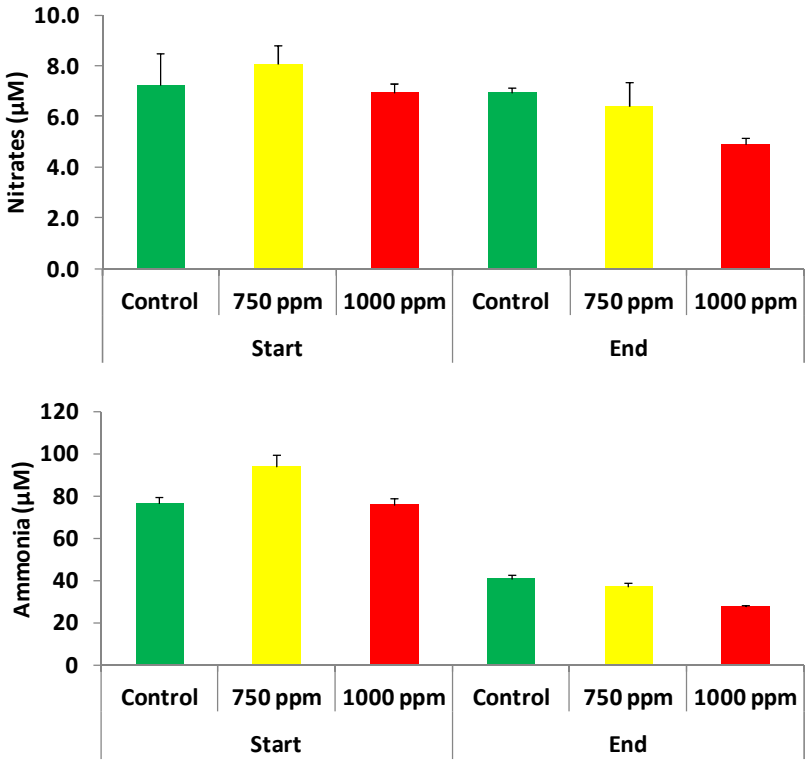

Figure S3. Variations in the concentration of nitrates and ammonia in the mesocosms during the experiment. Green = pH 8.08 (control); yellow = pH 7.88; red = pH 7.77

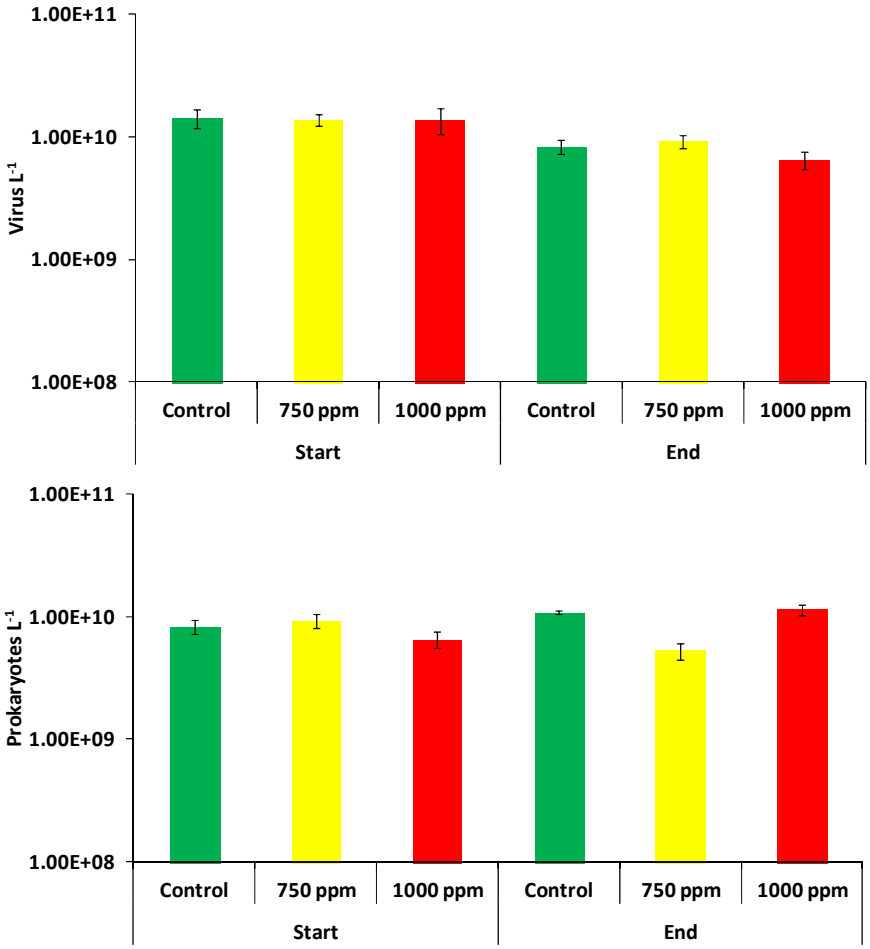

Figure S4. Changes in the abundance of prokaryotes and viruses during the incubation experiments. Green = pH 8.08 (control); yellow = pH 7.88; red = pH 7.77

Section 2 - Red coral growth rates

A buoyant weighing method was used[23,24] to estimate the colonies' net growth rates as calcification/dissolution rates under experimental conditions. Each weighting session was preceded by weighting of a standard weight in the air and in the water to correct for potential effect of water density. Each measure on the coral fragments was done in duplicate, with a verified maximum CV% between replicated measurements of 0,25%. The buoyant weighing method for estimating dry $CaCO_3$ weight was calibrated by plotting coral colonies final buoyant weight against their axial skeleton final dry $CaCO_3$ weight and against their total dry skeleton weight, i.e., axial skeleton plus sclerites (r=0.98 and 0.99, respectively; P<0.01 for all relationships, Figure S5a,b). This allowed to verify an error not exceeding 4% of coral skeleton dry weight when calculating red coral growth using buoyant weight method.

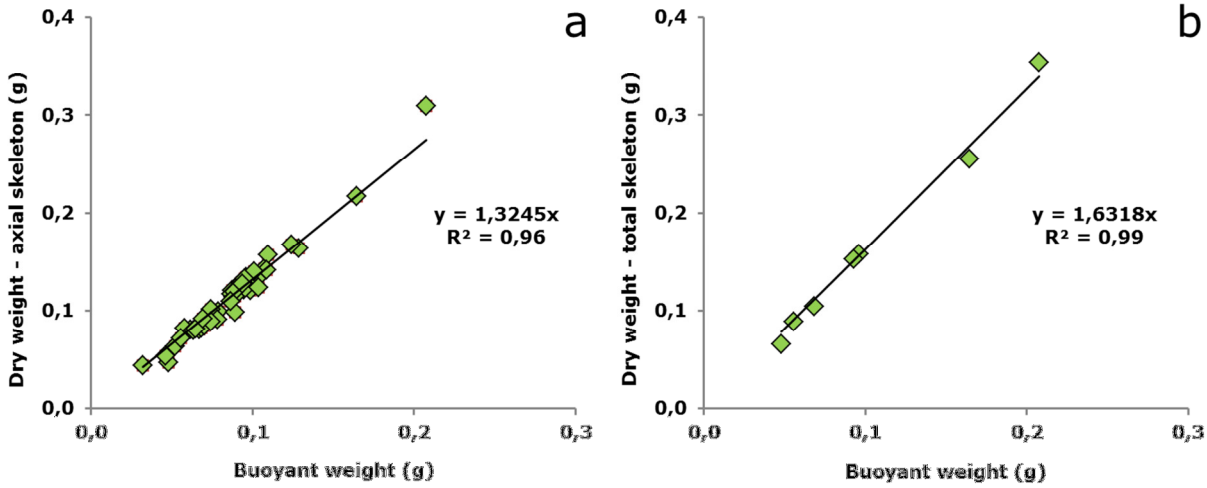

Figure S5. Relationship between colonies' buoyant weight and axial skeleton dry weight (a), and between colonies' buoyant weight and total skeleton dry weight, i.e., scleraxis plus sclerites (b).

The assessment of the annual growth rate of red coral colonies is essential to assign them to different age classes and to determine the age structure of a population. The available data on age and growth in red coral (Table S2) have been obtained using three different approaches: 1) petrographic method[25,26]; 2) staining of thin sections of the organic matrix from the base of colonies[27,28], which allows one to read annual growth rings; 3) direct measurements of new settled colonies of known age, a not destructive approach to the study of colony growth rate, based on artificial or semi-natural substrates on which new settled colonies can be followed during their growth for a determined time interval[29-31].

A recent paper suggested that the petrographic method underestimates age and thus overestimates growth rates of colonies[27]. The mean growth rate reported there was in fact 2.6 to 4.5 times lower than the growth rates based on the petrographic method (i.e., between 0.91 and 1.57 mm year^{-1}) in shallow and relatively deep habitats[25,26,32]. Taking into account that colonies analyzed in that study[27] came from an exploited population, in non-harvested ones red coral colonies could reach sizes notably larger and longevity could easily be 200 years[6].

Table S2. Overview of basal diameter growth rates of *C. rubrum* in past literature, according to the method used.

Location	Growth rate (mm y^{-1})	Study method	Reference
Cap de Creus, Spain	1.32	Petrographic method	García-Rodríguez & Massò[19]
Calafuria, Italy	0.91	Petrographic method	Santangelo *et al.*[20]
Calafuria, Italy	1.57	Petrographic method	Santangelo *et al.*[26]
NW Mediterranean	0.35 ± 0.15	Organic matrix staining	Marschal *et al.*[21]
Portofino MPA, Italy	0.22 ± 0.04	Organic matrix staining	Vielmini *et al.*[22]
Cap de Creus, Spain	0.24 ± 0.06	Organic matrix staining	Vielmini *et al.*[22]
Corsica, France	0.20	Organic matrix staining	Gallmetzer *et al.*[27]
Calafuria, Italy	0.62 ± 0.19	Direct measurements	Bramanti *et al.*[25]
Marseille, France	0.24 ± 0.05	Direct measurements	Garrabou & Harmelin[24]
Portofino MPA, Italy	0.94	Direct measurements	Cattaneo-Vietti *et al.*[28]
Portofino MPA, Italy	0.62	Direct measurements	Cerrano *et al.*[23]
Calafuria, Italy	0.68 ± 0.02	Direct measurements	Santangelo *et al.*[29]
Elba, Italy	0.59 ± 0.19	Direct measurements	Santangelo *et al.*[29]
Portofino, Italy (Lab)	0.45 ± 0.11	Buoyant weight technique	Control, present study
Portofino, Italy (Lab)	0.37 ± 0.08	Buoyant weight technique	pH 7.88, present study
Portofino, Italy (Lab)	0.33 ± 0.08	Buoyant weight technique	pH 7.77, present study

Growth rates calculated here through the equation (1)[25,33] are consistent with the available literature (Table S2). Recent studies tend towards growth rates between 0.24 and 0.68, but earlier estimates measured values up to 1.57 mm year^{-1} growth in basal diameter and values of growth rate similar to those reported here were obtained for red coral colonies collected from Portofino Marine Protected Area (i.e., the sampling site). The differences in conditions between habitats lead to inevitable variations in growth rate. Moreover, the controlled conditions of the experiment and the characteristics of the Portofino MPA, as it is a preserved coast with favourable trophic conditions, makes the found growth rate of 0.45 mm year^{-1} a credible value. The same analyses, made on specimen reared under acidified conditions, revealed a percentage reduction in growth rate of 18% and 45% from the control, for pH of

7.88 and 7.77 respectively. These growth rates remain close to the lower limits of the range of values reported from literature, and the reduction from the control gives evidence of the strong effect that ocean acidification can cause on the growth rates of this vulnerable species.

Section 4 - Statistical analyses

Table S3. Results of the one-way ANOVA with repeated measures testing for differences among treatments in colonies' buoyant weight during different phases and the entire duration of the experiment. Asterisks indicate: *, P < 0.05; **, P < 0.01; ***, P < 0.001. ns, not significant.

Days	Source	DF	Sum of quadrats	Mean squares	F	P
0-10	**Treatment**	2	0.0816	0.041	49.51	***
	Error	6	0.0049	0.001		
	Total	8	0.0866			
10-30	**Treatment**	2	0.0003	0.000	6.20	*
	Error	6	0.0001	0.000		
	Total	8	0.0004			
30-45	**Treatment**	2	0.0390	0.019	41.73	***
	Error	6	0.0028	0.000		
	Total	8	0.0418			
0-45	**Repetition (Time)**	2	0.115	0.057	180.52	***
	Treatment x Repetition	4	0.046	0.011	35.96	***
	Error	12	0.004	0.000		

Pairwise tests	
Contrast: Treatment	**P**
Control (8.08 pH) > 7.88 pH	**
Control (8.08 pH) > 7.77 pH	**
7.88 pH < 7.77 pH	ns

The effects of acidification on colonies' buoyant weight, relative abundance of fluorescent capstan and cross sclerites and values of the fluorescent cross to capstan sclerites ratio were assessed, separately for each variable, using one-way analysis of variance, testing for differences encountered among treatments, with n=15 (Table S4 and S5). Before the analyses, the homogeneity of variances was checked using the Cochran's test. The effect of variability among mesocosms assigned to each treatment was not considered here, as all the analyses of variance conducted including the different mesocosms as an explanatory factor indicated that this potential source of variability was always not significant.

Table S4. Results of the one-way ANOVA testing for differences among treatments for relative abundance of fluorescent capstans (A) and crosses (B) and values of the fluorescent cross to capstan ratio (C). Asterisks indicate: *, P < 0.05; **, P < 0.01; ***, P < 0.001. ns, not significant.

(A) one-way ANOVA: newly-accreted capstans				
Source	**df**	**MS**	**Pseudo-F**	**P**
Treatment	2	4.9E-01	347.5	***
Residual	42	1.4E-03		
Total	44			
Pairwise test				
Contrast: Treatment			**P**	
Control (8.08 pH) > 7.88 pH			**	
Control (8.08 pH) > 7.77 pH			**	
7.88 pH = 7.77 pH			ns	
(B) one-way ANOVA: newly-accreted crosses				
Source	**df**	**MS**	**Pseudo-F**	**P**
Treatment	2	1.1E-01	27.5	***
Residual	42	4.0E-03		
Total	44			
Pairwise test				
Contrast: Treatment			**P**	
8.08 > 7.88			**	
8.08 > 7.77			**	
7.88 = 7.77			ns	
(C) one-way ANOVA: newly-accreted cross/capstan				
Source	**df**	**MS**	**Pseudo-F**	**P**
Treatment	2	2.5E-02	3.4	*
Residual	42	7.1E-03		
Total	44			
Pairwise test				
Contrast: Treatment			**P**	
Control (8.08 pH) = 7.88 pH			ns	
Control (8.08 pH) < 7.77 pH			*	
7.88 pH = 7.77 pH			ns	

Table S5. Results of the analysis of variance with repeated measures testing for changes in polyps' activity and percentage of open polyps during the experiment. ***, P < 0.001. ns, not significant.

Variable	Source	DF	Sum of squares	Mean of squares	F	P
Polyps' activity	**Repetition (time)**	37	33904.5	916.3	93.21	***
	Treatment x Time	74	14045.8	189.8	19.31	***
	Error	222	2182.5	9.8		
Open polyps	**Repetition (time)**	37	21389.8	578.1	189.83	***
	Treatment x Time	74	2697.2	36.4	11.97	***
	Error	222	676.1	3.0		

Pairwise tests	
Contrast: Treatment	**P**
Control (8.08 pH) > 7.88 pH	*
Control (8.08 pH) > 7.77 pH	**
7.88 pH < 7.77 pH	ns

Supplementary references

1 Tsounis, G. *et al.* The Exploitation and Conservation of Precious Corals. *Oceanogr. Mar. Biol. Annu. Rev.* **48**, 161-212 (2010).

2 Cairns, S. D. Deep-water corals: An overview with special reference to diversity and distribution of deep-water scleractinian corals. *Bull. Mar. Sci.* **81**, 311-322 (2007).

3 Lumsden, S. E., Hourigan, T. F., Bruckner, A. W. & Dorr, G. *The state of deep coral ecosystems of the United States*. (NOAA Technical Memorandum CRCP-3, Silver Spring, MD, 2007).

4 Hughes, T. P. Catastrophes, phase shifts, and large-scale degradation of a Caribbean coral reef. *Science* **265**, 1547-1551 (1994).

5 Ballesteros, E. Mediterranean coralligenous assemblages: A synthesis of present knowledge. *Oceanogr. Mar. Biol. Annu. Rev.* **44**, 123-195 (2006).

6 Teixidó, N., Garrabou, J. & Harmelin, J. G. Low dynamics, high longevity and persistence of sessile structural species dwelling on mediterranean coralligenous outcrops. *PLoS ONE* **6**, e23744, doi:10.1371/journal.pone.0023744 (2011).

7 Costantini, F. *et al.* Deep-water *Corallium rubrum* (L., 1758) from the Mediterranean Sea: Preliminary genetic characterisation. *Mar. Ecol.* **31**, 261-269 (2010).

8 Dauphin, Y. Mineralizing matrices in the skeletal axes of two *Corallium* species (Alcyonacea). *Comp. Biochem. Physiol. Part A Mol. Integr. Physiol.* **145**, 54-64 (2006).

9 Debreuil, J. *et al.* Comparative analysis of the soluble organic matrix of axial skeleton and sclerites of *Corallium rubrum*: Insights for biomineralization. *Comp. Biochem. Physiol. Part B Biochem. Mol. Biol.* **159**, 40-48 (2011).

10 Cvejic, J. *et al.* Determination of canthaxanthin in the red coral (*Corallium rubrum*) from Marseille by HPLC combined with UV and MS detection. *Mar. Biol.* **152**, 855-862 (2007).

11 Vielzeuf, D., Garrabou, J., Baronnet, A., Grauby, O. & Marschal, C. Nano to macroscale biomineral architecture of red coral (*Corallium rubrum*). *Am. Min.* **93**, 1799-1815 (2008).

12 Vielzeuf, D. *et al.* Multilevel modular mesocrystalline organization in red coral. *Am. Min.* **95**, 242-248 (2010).

13 Floquet, N. & Vielzeuf, D. Mesoscale twinning and crystallographic registers in biominerals. *Am. Min.* **96**, 1228-1237 (2011).

14 Allemand, D. & Grillo, M. C. Biocalcification mechanisms in gorgonians. ^{45}Ca uptake and deposition by the mediterranean red coral *Corallium rubrum*. *J. Exp. Zool.* **292**, 237-246 (1992).

15 Grillo, M. C., Goldberg, W. M. & Allemand, D. Skeleton and sclerite formation in the precious red coral *Corallium rubrum*. *Mar. Biol.* **117**, 119-128 (1993).

16 Allemand, D. The biology and skeletogenesis of the Mediterranean Red Coral: a review. *Precious Corals Octocoral Res.* **2**, 19-39 (1993).

17 Dickson, A. G., Sabine, C. L. & Christian, J. R. *Guide to best practices for ocean CO_2 measurements*. Vol. 3 (PICES Special Publication, 2007).

18 Rivaro, P., Messa, R., Massolo, S. & Frache, R. Distributions of carbonate properties along the water column in the Mediterranean Sea: Spatial and temporal variations. *Mar. Chem.* **121**, 236-245 (2010).

19 Chisholm, J. R. M. & Gattuso, J. P. Validation of the alkalinity anomaly technique for investigating calcification and photosynthesis in coral reef communities. *Limnol. Oceanogr.* **36**, 1232-1239 (1991).

20 Riebesell, U., Fabry, V. J., Hansson, L. & Gattuso, J. P. *Guide to Best Practices for Ocean Acidification Research and Data Reporting* (Publications Office of the European Union, Luxembourg, 2010).

21 Cohen, A. L. & Holcomb, M. Why corals care about ocean acidification: uncovering the mechanism. *Oceanogr.* **22**, 118-127 (2009).

22 Chauvin, A., Denis, V. & Cuet, P. Is the response of coral calcification to seawater acidification related to nutrient loading? *Coral Reefs* **30**, 911-923 (2011).

23 Davies, P. S. A rapid method for assessing growth rates of corals in relation to water pollution. *Mar. Poll. Bull.* **21**, 346-348 (1990).

24 Ferrier-Pagès, C., Gattuso, J. P., Dallot, S. & Jaubert, J. Effect of nutrient enrichment on growth and photosynthesis of the zooxanthellate coral Stylophora pistillata. *Coral Reefs* **19**, 103-113 (2000).

25 García-Rodríguez, M. & Massò, C. Estudio biométrico de poblaciones de coral rojo (*Corallium rubrum* L.) del litoral de Gerona (NE de España). *Bol. Inst. Esp. Oceanogr.* **3**, 61-64 (1986).

26 Santangelo, G., Abbiati, M. & Caforio, G. in *Red coral in the Mediterranean Sea: art, history and science* (eds F. Cicogna & R. Cattaneo-Vietti) 131-157 (Min. Ris. Agr. Al. For., Rome, 1993).

27 Marschal, C., Garrabou, J., Harmelin, J. G. & Pichon, M. A new method for measuring growth and age in the precious red coral *Corallium rubrum* (L.). *Coral Reefs* **23**, 423-432 (2004).

28 Vielmini, I. *et al.* in *International Workshop on Red Coral Science, Management, and Trade: Lessons from the Mediterranean.* (eds E. Bussoletti *et al.*) 179-182 (NOAA Technical Memorandum CRCP-13, Silver Spring, MD, 2010).

29 Cerrano, C., Bavestrello, G., Cicogna, F. & Cattaneo, R. in *Red Coral and Other Octocorals: Biology and Protection* (eds F. Cicogna, G. Bavestrello, & R. Cattaneo) 57-73 (Min. Pol. Agr., Rome, 1999).

30 Garrabou, J. & Harmelin, J. G. A 20-year study on life-history traits of a harvested long-lived temperate coral in the NW Mediterranean: Insights into conservation and management needs. *J. Anim. Ecol.* **71**, 966-978 (2002).

31 Bramanti, L., Magagnini, G., De Maio, L. & Santangelo, G. Recruitment, early survival and growth of the Mediterranean red coral *Corallium rubrum* (L 1758), a 4-year study. *J. Exp. Mar. Biol. Ecol.* **314**, 69-78 (2005).

32 Santangelo, G., Bongiorni, L., Giannini, F., Abbiati, M. & Buffoni, G. in *Red Coral and Other Mediterranean Octocorals: Biology and Protection* (eds F. Cicogna, G. Bavestrello, & R. Cattaneo-Vietti) 23-43 (Min. Ris. Agr. Al. For., Rome, 1999).

33 Tsounis, G., Rossi, S., Gili, J. M. & Arntz, W. E. Red coral fishery at the costa brava (NW Mediterranean): Case study of an overharvested precious coral. *Ecosystems* **10**, 975-986 (2007).